EUROPHYSICS LETTERS 15 December 2003

Europhys. Lett., **64** (6), pp. 810–815 (2003)

Concentric domains in patterned thin films with perpendicular magnetic anisotropy

Jonathan Kin Ha, Riccardo Hertel and J. Kirschner

Max-Planck-Institut für Mikrostrukturphysik - Weinberg 2, 06120 Halle, Germany

(received 4 June 2003; accepted 13 October 2003)

PACS. 75.70.Kw – Domain structure (including magnetic bubbles).
PACS. 75.75.+a – Magnetic properties of nanostructures.
PACS. 02.70.Dh – Finite-element and Galerkin methods.

Abstract. – We report a finite-element micromagnetic study on domain structures in tetragonally distorted Ni(001) films which are confined to the geometric shapes of a cylindrical disc, rectangular and triangular prisms, and a pacman. The thickness-dependent perpendicular anisotropy is provided by the inverse magnetostriction effect. It is found that some of the observed perpendicular domain patterns reflect the in-plane shape of their respective element. We call these domains "concentric domains". The geometric effect on the domain shape is attributed to the inhomogeneity of the demagnetizing field.

Introduction. – Patterned magnetic thin films have attracted much attention from both theoreticians and experimentalists in the past five years for at least two reasons: i) they provide a unique opportunity to study the effect of lateral confinement on the spin arrangements as well as on the magnetization processes [1–7]; ii) they are a potential candidate for high-density and fast-switching recording [8,9]. So far, much of the effort has been devoted to soft magnetic materials such as permalloy and iron in which the magnetization lies predominately in the film plane. The effect of lateral confinement on a perpendicular medium has hardly been addressed. The reason for the lack of research in this area is perhaps due to its unapparent nature: while it is clear that the in-plane magnetization tends to align with the sample geometric curvature to minimize magnetic surface charges([1]), it is not evident whether the out-of-plane component can sense the lateral confinement, since it does not create magnetic poles at the lateral surface. The goal of the present work is to show that the shape can have a decisive impact on the domain structure of a thin-film element with a perpendicular magnetic anisotropy. More specifically, it will be argued that the demagnetizing field of a uniformly magnetized state along the film normal direction favors the fragmentation of the single perpendicular domain into "concentric domains", each of which mimics the in-plane geometric shape of the element. Concentric domains will be demonstrated in various geometric shapes using a finite-element micromagnetic technique (see fig. 1).

([1])For example, the magnetization of the vortex state in a permalloy or supermalloy disk follows the disc circular curvature very closely to avoid creating magnetic poles at the disc perimeter as much as possible [1,4].

© EDP Sciences

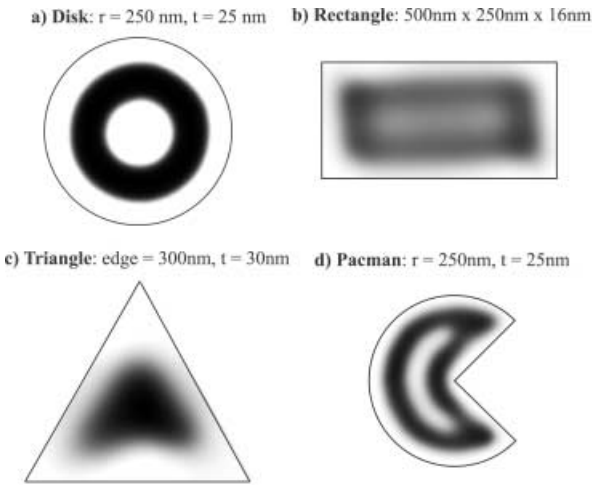

Fig. 1 – Domain structures of tetragonally distorted nickel in four different geometries: a) cylindrical disc; $Q = 0.94$; b) rectangular prism; $Q = 0.68$; c) triangle; $Q = 0.59$; d) pacman; $Q = 0.67$. Here, $Q = \frac{(K_\mathrm{u}+2K_\mathrm{s}/t)}{K_d}$, where K_u is the uniaxial anisotropy coefficient, $K_d = J_\mathrm{s}^2/2\mu_0$ is the stray field constant, and K_s the Néel surface constant. The gray scale reflects the out-of-plane component of the magnetization: white = up; black = down.

Material parameters and numerical method. – Tetragonally distorted fcc-Ni(001) films are the chosen material for the present investigation. The biaxial tensile strain in the nickel layer can provide a strong perpendicular anisotropy because bulk nickel is a highly negative magnetostrictive material among the 3*d* transition metals and their alloys. For example, the nickel in the Cu/Ni/Cu(001) system has been shown to exhibit an out-of-plane easy axis of magnetization for a wide range of film thicknesses: $3\,\mathrm{nm} \leq t \leq 12\,\mathrm{nm}$ [10–13]; and for thicker films ($t > 70\,\mathrm{nm}$), ripple domains are also observed [14, 15]. In this study, the strain in the nickel layer is modelled to be uniform and decrease with increasing film thickness. More specifically, it is taken to have a $t^{-2/3}$ behavior as found by Ha *et al.* [16] in their Cu/Ni/Cu(001) stacks([2]). In addition, the two nickel interfaces are assumed to be identical in the calculation, though this may not be realizable in an actual experiment because of the growth asymmetry even with the same material. The saturation magnetic polarization J_s used in the calculation is 0.61 tesla with the exchange stiffness constant $A = 1.0 \times 10^{-11}\,\mathrm{J/m}$.

The numerical method is based on Brown's principles of static micromagnetics. The calculation is done using finite elements combined with the boundary integral method or FEM-BEM. The energy of the system is modelled to consist of the exchange, stray field, uniaxial perpendicular anisotropy which is provided by the inverse magnetostriction effect, and the Néel-surface term. A stable magnetic configuration is obtained by seeking a minimum in the total energy by means of self-consistency; that is, the demagnetizing field is first calculated using an assumed magnetic configuration which is allowed to relax in the presence of this same stray field. It is then re-calculated from the new minimum-energy configuration. The whole process repeats until a self-consistent solution is obtained. A more detailed discussion of the numerical method can be found in ref. [17].

([2])In reality, the strain is certainly not uniform. Further, the actual strain state of the tetragonally distorted nickel layer is quite sensitive to the growth conditions and even the thickness of the capping layer [13].

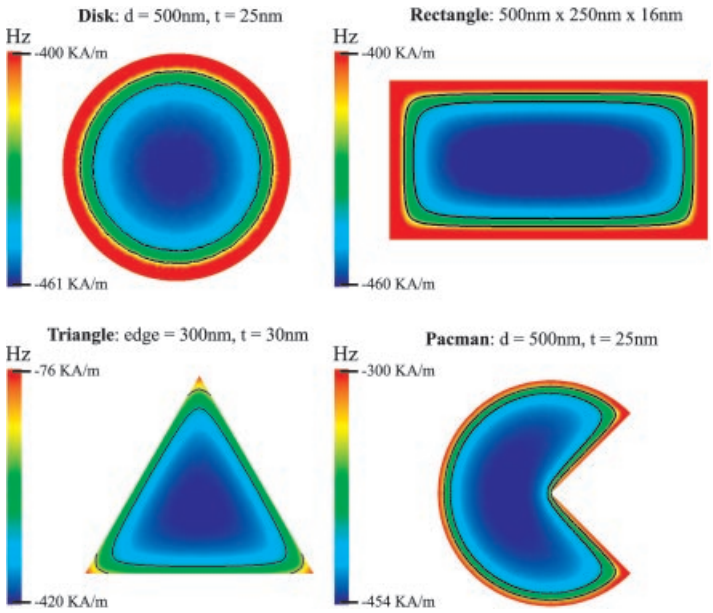

Fig. 2 – Contour plots of H_z (the normal component of the demagnetizing field) in the four geometries when the magnetization is fully out of plane. They are cross-sectional views of the central planes parallel to the surface of each respective element. The solid lines are the contour lines (lines of constant H_z).

Numerical results. – Figure 1 shows stable domain structures of the nickel films confined to the geometric shapes of a cylindrical disc, rectangular and triangular prisms, and a pacman. These domain structures are obtained by allowing a uniform perpendicular magnetization to relax to an energy-minimum configuration in the absence of a magnetic field. The observed patterns are ordered bands of alternating up and down domains. The shape of each band reflects the in-plane geometry of their respective element: circular domains in the disc, rectangular domains in the rectangular prism, and so forth. Because these domains share a common center (more or less) in the element, they are thereby referred to as concentric domains. The

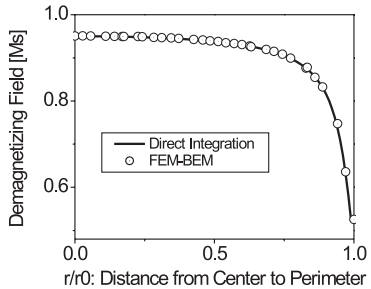

Fig. 3 – The line profile of H_z from the center to the perimeter of the disk ($r = 250\,\text{nm}$, $t = 25\,\text{nm}$). The line of circles is the result from our micromagnetic code. The solid line is obtained by directly integrating the surface charges as discussed in footnote ([3]). The magnetization is assumed uniform along the cylindrical long or z-axis. r_0 is the radius of the disk.

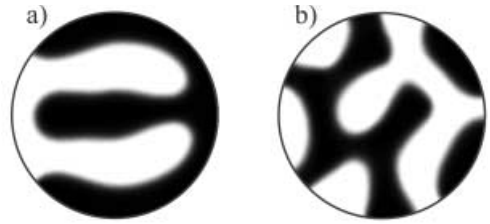

Fig. 4 – Random band domains in the disk with diameter of 500 nm, thickness 25 nm. The gray scale corresponds to the out-of-plane component of the magnetization: white = up; black = down. a) The starting configuration is two oppositely magnetized perpendicular domains; b) a random demagnetized state. The uniaxial and surface anisotropy coefficients used in the calculation are: $K_{\mathrm{u}} = 8.3 \times 10^4\,\mathrm{J/m^3}$; $K_{\mathrm{s}} = 7 \times 10^{-4}\,\mathrm{J/m^2}$.

number of concentric bands that can be supported in an element depends strongly on its size: the larger the element, the more bands it can accommodate. The exact number is the result of the balance between the need to minimize the stray field and domain-wall energy. In some elements, the magnetization in a domain may not fully point out of the film plane, as this is the case for the one at the center of the rectangular prism ($M_z/M_s = -0.54$). The degree of canting reflects the compromise among the various energy terms, namely the stray field, exchange, bulk and surface anisotropies. Lastly, it is interesting to see the sharp corners of the prisms and pacman appear smoother in the domains, as this would be expected because any drastic variation in the magnetization would cost too much exchange energy.

Discussion. – Though the concentric ring domain structure has been observed in the literature [18–20], no clear explanations were given as to how the out-of-plane component of the magnetization senses the in-plane geometric confinement. Since domain formation is usually the result of the need to minimize the stray field energy, it is reasonable to begin the inquiry by examining the demagnetizing field of the initial state.

Figure 2 shows the contour plot of the normal component of the demagnetizing field H_z for each of the elements discussed above, when they are fully magnetized perpendicular to the film plane. These are cross-sectional views of the central plane parallel to the film surface of their respective element. The color contrast reflects the non-uniform nature of the demagnetizing field, as one would expect from a non-ellipsoidal element [21–23]. For a more in-depth look at the field profile, fig. 3 shows the magnitude of H_z as a function of position from the center to the perimeter of the disk([3]). The plot reveals that the demagnetizing field is weakest at the perimeter and strongest at the center. This is because there are less magnetic surface charges to generate the field near the in-plane boundary. More quantitatively, there is a difference of 223 kA/m or 2802 Oe, which says that the magnetization at the perimeter is much more firmly held out-of-plane than that in the interior by the anisotropy field because the former

([3])Two estimates of the profile are given: one (the line of circles) is our result from our micromagnetic code; the other (the solid line) is obtained by directly integrating the following integral over the magnetic charges at the top and bottom surfaces [24]:

$$H_z(\vec{r}) = \frac{M_{\mathrm{s}}}{4\pi} \int_{\mathrm{Surf}} \frac{(z' - z) n_{z'}}{\left|\vec{r'} - \vec{r}\right|^3} \mathrm{d}x'\,\mathrm{d}y'.$$

Here, the z-axis is taken to be along the disk normal direction, $n_{z'}$ is the z'-component of the surface unit vector ($n_{z'} = 1$ or -1 for the top and bottom surfaces, respectively). Obviously, the two results are in good agreement. Their comparison gives a confirmation that the demagnetizing field is correctly calculated in the micromagnetic program.

is subjected less to the demagnetizing effect. This field difference in the demagnetizing field, combined with the fact that the contour lines of H_z (the solid lines in fig. 2) have the in-plane symmetry of the element shape —radial symmetry in the disk, 3-fold symmetry in the triangle, and so forth— make the concentric domains structure more *accessible* over other stable magnetic configurations.

To elucidate the favoring of the concentric domain state by the demagnetizing field, let us examine the fragmentation process from the point of view of energy minimization. Starting from a uniformly magnetized state along the disk normal direction, the single-domain state would find it energetically more favorable to break into a multiple-domain structure to save the stray-field energy. But the fragmentation process is not likely to occur at the boundary because there the magnetization is firmly held out of plane for the reason discussed above. Instead, pocket(s) of opposite domain will form in the disk interior and evolve in such a way as to provide an efficient way to close the flux field generated by the outermost domain. In other words, the geometry-adopted variation of the demagnetizing field paves the way for the formation of the concentric domains. Though not shown in this paper, an examination of the in-between states during the minimization process gives a confirmation to the above argument.

The whole argument for the observation of concentric domains hinges on the starting configuration being uniformly magnetized in the film normal direction. If this is not the case, they may not be as accessible, simply because the spatial variation of the normal component of the demagnetizing field no longer follows the element shape. Hence there would be no "template" from which the fragmentation process is to begin. This intuition is indeed confirmed by our simulations. For example, if the starting configuration is a total random state (that is, a state in which the magnetization is randomly distributed in the element) or a state in which half of the disk is magnetized up, the other down, the resulting domain structure is that of random band domains, as shown in fig. 4.

In short, the lateral geometric confinement on the Ni(001) films has been shown to have a significant impact on their domain structures. More specifically, concentric domains can be observed provided the sample is allowed to relax from an initial saturated state along the film normal direction. The key factor to understand this effect lies in the way in which the demagnetizing field varies spatially in the element. As a final remark, it is important to mention that the fct-Ni(001) system is just a good example by which the lateral confinement effect discussed above can be illustrated. It is by no means the only system in which the phenomenon of concentric domains can be observed.

REFERENCES

[1] Cowburn R. P., Koltsov D. K., Adeyeye A. O., Welland M. E. and Tricker D. M., *Phys. Rev. Lett.*, **83** (1999) 1042.
[2] Cowburn R. P., *J. Phys. D*, **33** (2000) R1.
[3] Schneider M., Hoffmann H., Otto S., Haug Thu. and Zweck J., *J. Appl. Phys.*, **92** (2002) 1466.
[4] Jonathan K. Ha, Riccardo Hertel and Kirschner J., *Phys. Rev. B*, **67** (2003) 224432.
[5] Wachowiak A., Wiebe J., Bode M., Pietzsch O., Morgenstern M. and Wiesendanger R., *Science*, **298** (2002) 577.
[6] Schabes M. E. and Bertram H. N., *J. Appl. Phys.*, **64** (1988) 1347.
[7] Jonathan Kin Ha, Riccardo Hertel and Kirschner J., *Phys. Rev. B*, **67** (2003) 064418.
[8] Jacques Ferré, *Dynamics of Magnetization Reversal: From Continuous to Patterned Ferromagnetic Films*, edited by Hillebrands B. and Ounadjela K. (Springer) 2002, p. 127.
[9] Randall Victora, *The Physics of Ultra-High-Density Magnetic Recording*, edited by Plumer M. L., van Ek J. and Weller D., Perpendicular Recording Media (Springer) 2001, p. 230.

[10] Jungblut R., Johnson M. T., aan de Stegge J., Reinders A. and den Broeder F. J. A., *J. Appl. Phys.*, **75** (1994) 6424.
[11] Gabriel Bochi, Ballentine C. A., Inglefield H. E., Thompson C. V. and O'Handley R. C., *Phys. Rev. B*, **53** (1996) R1729.
[12] Kin Ha and O'Handley R. C., *J. Appl. Phys.*, **85** (1999) 5282.
[13] Keiki Fukumoto, Hiroshi Daimon, Liviu Chelaru, Francesco Offi, Wolfgang Kuch and Jürgen Kirschner, *Surf. Sci.*, **514** (2002) 151.
[14] Hameed S., Talagala P., Naik R., Wenger L. E., Naik V. M. and Proksch R., *Phys. Rev. B*, **64** (2001) 184406.
[15] Ciria M., Arnaudas J. I., Benito L., de la Fuente C., del Moral A., Ha J. K. and O'Handley R. C., *Phys. Rev. B*, **67** (2003) 024429.
[16] Ha K., Ciria M., O'Handley R. C., Stephens P. W. and Pagola S., *Phys. Rev. B*, **60** (1999) 13780.
[17] Riccardo Hertel, *J. Appl. Phys.*, **90** (2001) 5752.
[18] Michel Hehn, Kamel Ounadjela, Jean-Pierre Bucher, Françoise Rousseaux, Dominique Decanini, Bernard Bartenlian and Claude Chappert, *Science*, **272** (1996) 1782.
[19] Ignatchenko V. A. and Mironov E. Yu., *J. Magn. & Magn. Mater.*, **124** (1993) 315.
[20] Buda L. D., Prejbeanu I. L., Demand M., Ebels U. and Ounadjela K., *IEEE Trans. Magn.*, **37** (2001) 2061.
[21] Amikam Aharoni, *Introduction to the Theory of Ferromagnetism* (Oxford Science Publications) 1996.
[22] Aharoni A., *Phys. Status Solidi B*, **229** (2002) 1413.
[23] Guobao Zheng, Pardavi-Horvath M. and Xiaohau Huang, *J. Appl. Phys.*, **79** (1996) 5742.
[24] Ernst Schlömann, *J. Appl. Phys.*, **33** (1962) 2825.